Biosensors and Bioelectronics 34 (2012) 165–170

Contents lists available at SciVerse ScienceDirect

Biosensors and Bioelectronics

journal homepage: www.elsevier.com/locate/bios

An aptamer based competition assay for protein detection using CNT activated gold-interdigitated capacitor arrays

Anjum Qureshi [a,b], Irena Roci [b], Yasar Gurbuz [b], Javed H. Niazi [a,*]

[a] Sabanci University Nanotechnology Research and Application Center, Orta Mahalle, Tuzla 34956, Istanbul, Turkey
[b] Faculty of Engineering and Natural Sciences, Sabanci University, Orhanli 34956, Tuzla, Istanbul, Turkey

ARTICLE INFO

Article history:
Received 8 December 2011
Received in revised form 20 January 2012
Accepted 27 January 2012
Available online 6 February 2012

Keywords:
Label-free
Aptamers
C-reactive protein
Carbon nanotubes
Capacitive biosensor
Affinity assay

ABSTRACT

An aptamer can specifically bind to its target molecule, or hybridize with its complementary strand. A target bound aptamer complex has difficulty to hybridize with its complementary strand. It is possible to determine the concentration of target based on affinity separation system for the protein detection. Here, we exploited this property using C-reactive protein (CRP) specific RNA aptamers as probes that were immobilized by physical adsorption on carbon nanotubes (CNTs) activated gold interdigitated electrodes of capacitors. The selective binding ability of RNA aptamer with its target molecule was determined by change in capacitance after allowing competitive binding with CRP and complementary RNA (cRNA) strands in pure form and co-mixtures (CRP:cRNA = 0:1, 1:0, 1:1, 1:2 and 2:1). The sensor showed significant capacitance change with pure forms of CRP/cRNA while responses reduced considerably in presence of CRP:cRNA in co-mixtures (1:1 and 1:2) because of the binding competition. At a critical CRP:cRNA ratio of 2:1, the capacitance response was dramatically lost because of the dissociation of adsorbed aptamers from the sensor surface to bind when excess CRP. Binding assays showed that the immobilized aptamers had strong affinity for cRNA (K_d = 1.98 μM) and CRP molecules (K_d = 2.4 μM) in pure forms, but low affinity for CRP:cRNA ratio of 2:1 (K_d = 8.58 μM). The dynamic detection range for CRP was determined to be 1–8 μM (0.58–4.6 μg/capacitor). The approach described in this study is a sensitive label-free method to detect proteins based on affinity separation of target molecules that can potentially be used for probing molecular interactions.

1. Introduction

Identification and characterization of molecular interactions is important in designing novel assays for biosensing. A number of methodologies have been established in recent years to probe molecular interactions (Berezovski and Sergey 2003; Foulds and Etzkorn, 1998; Pagano et al., 2011; Royer and Scarlata, 2008; Ryder et al., 2008; Wan and Le, 2000; Wong and Lohman, 1993). These interactions occur at the molecular interfaces and they are mainly electrostatic in nature. Various methods were employed to monitor formation of protein/nucleic acid complexes. These include the optical method, such as Surface Plasmon Resonance methods, fluorescent approaches, and others such as, electrophoretic mobility shift assays, affinity capillary electrophoresis and nitrocellulose-filter binding assays (Berezovski and Sergey, 2003; Foulds and Etzkorn, 1998; Karlsson, 2004; Pagano et al., 2011; Ryder et al., 2008; Singhal and Otim, 2000; Wan and Le, 2000). In addition, label-free methods, such as non-Faradaic type can also be employed by immobilizing biological receptors on the surface of a suitable electronic transducer, which converts the molecular interaction signal into a quantifiable electronic signal.

Until now, the different nature of nucleic acid recognition elements and their protein targets indicated great promise for designing innovative sensing protocols (Strehlitz et al., 2008). Synthetic oligonucleotides, called aptamers, have attracted much of attention because of their binding abilities similar to antibodies, as well as their relative ease of isolation, modification, tailored binding affinity, chemical synthesis and resistance against denaturation. These are short, single stranded DNA or RNA oligonucleotides that can bind to their targets and offer specific properties, which favor them for developing protein arrays, drug delivery and as new biorecognition elements for biosensing of disease-related proteins (Bagalkot et al., 2006; Hansen et al., 2006; Mukhopadhyay, 2005; Strehlitz et al., 2008). Aptamers are typically generated by an iterative screening process of complex synthetic nucleic acid libraries against specific target molecules, making them more specific to target molecules. The targets can be ions, small organic molecules, proteins or even whole cells. The molecular interactions derived from their interaction with target molecules generally follow natural rules of biomolecular interactions.

Most of the aptamer based assays were designed to detect specific proteins as disease markers and rely on standard sandwich

* Corresponding author. Tel.: +90 216 483 9879; fax: +90 216 483 9885.
E-mail address: javed@sabanciuniv.edu (J.H. Niazi).

0956-5663/$ – see front matter © 2012 Elsevier B.V. All rights reserved.
doi:10.1016/j.bios.2012.01.038

type bio-affinity assays in connection to common enzyme (Xu et al., 2009), fluorophore (Wang et al., 2008) or nanoparticle tracers (Chiu and Huang, 2009). Until now, electrochemical aptamer-based biosensors, such as redox-mediating faradaic type or label-free direct measurement of charge distribution/capacitance by non-faradaic type have been reported on different platforms to detect specific disease biomarkers and cells using aptamers (Lei et al., 2009; Sassolas et al., 2009; Velasco-Garcia and Missailidis, 2009; Xu et al., 2009) or by using antibodies (de Vasconcelos et al., 2009; Laczka et al., 2008; Varshney et al., 2007).

CRP is one of the acute-phase plasma proteins under cardiovascular disease (CVD) conditions and serves as a target for early diagnosis and prevention of CVD. CRP has been regarded as low risk at a concentration below 1.0 mg/l, moderate for 1.0–3.0 mg/l, and high risk for concentrations over 3.0 mg/l (Pearson et al., 2003). It can rise as high as 1000-fold because of inflammation induced by infection/injury that often lead to CVD (Casas et al., 2008). Recently, a label-free capacitive biosensor for CRP detection has been reported from our laboratory that utilized antibodies (Quershi et al., 2009), which are prone to lose their activity over time and the advantages in relation to previous works is described in Supporting Information (SI) section 1. Therefore, synthetic aptamers made of ssDNA/RNA were employed as affinity ligands on capacitor arrays that are stable and specifically bind CRP. Studies pertinent to the binding affinity interactions of aptamers with target molecules by direct charge distribution are scarce. Therefore, here, a competitive assay was designed by utilizing RNA aptamers immobilized on capacitors and competitively assayed with different molar ratios of CRP (as a model protein) and cRNA. This study demonstrates that it is possible to determine the target concentration by affinity separation, which is facilitated by bound/free aptamer in presence of its complementary strand and the target by capacitive responses. The interaction events were captured based on charge distribution under the applied frequency using capacitors made of two electrodes for ground and signal in the absence of redox mediators. This method is effective for probing biomolecular binding events such as ligand–target interactions. The measuring principle of these sensors is based on simple changes in dielectric properties or charge distribution and conductivity when a ligand–target complex formed on the surface of an electrode without redox mediators (Gautier et al., 2007; Quershi et al., 2009; Tlili et al., 2005). The determinants of quantitative parameters of binding specificity, affinity and stoichiometry were measured.

2. Materials and methods

2.1. Materials and chemicals

Silicon wafers of 4″ size, <1 0 0> oriented, p-type with the resistivity of 9–12 Ω cm and thicknesses of 500 ± 25 μm and 1 μm thick SiO_2 layer on top were obtained from University Wafers, USA. Carboxy-functionlized multiwalled CNTs (carboxy-CNTs) were obtained from Arry®, Germany. Cysteamine, dimethyl sulfoxide (DMSO, 99.9%), 1-ethyl-3-[3-dimethylaminopropyl] carbodiimide hydrochloride (EDC) and *N*-hydroxysuccinimide (NHS) were purchased from Sigma–Aldrich, Germany. All RNA oligonucleotides were custom synthesized by Bioresearch Tech. Inc., USA, and a random ssDNA oligonucleotide was purchased from SynGen, Inc., USA.

2.2. Patterning gold interdigitated electrode (GID) array for fabrication of capacitor arrays

GID arrays were patterned on SiO_2 surface by image reversal photolithography. In this process, the metal layers were patterned using the dual tone photoresist AZ5214E. A 2 μm thick AZ5214E photoresist was patterned with the help of a mask for a lift-off process in pure acetone as a solvent. Following this step, the SiO_2 film was covered by a layer of 50–60 nm of tungsten (W) to improve the adhesion of gold, and then, a 200–210 nm layer of gold was deposited on W by DC sputtering method. The dimension of each electrode was 800 μm in length, 40 μm in width with a distance between two electrodes of 40 μm. Each sensor contained 24-interdigitated electrodes with a total area of 3 mm^2.

2.3. Immobilization of CNTs and RNA on sensor arrays

Steps involved in CNTs and RNA immobilization are schematically shown in Scheme S1 of the SI section 2. The sensor chip was first plasma cleaned and immersed in 1 mM cysteamine (prepared in 95% ethanol) for 24 h and was washed with ethanol and dried using N_2 gas. The self-assembled monolayer (SAM) of cysteamine formed on gold surface contained free NH_2 groups that were utilized for covalently attachment of carboxy-CNTs. For this, 100 μl of 1 mg/ml carboxy-CNTs suspension in DMSO was mixed with equal volume of 1:1 mixture of 200 mM of EDC and 100 mM NHS. The suspension was sonicated with alternative cycles of 10 s pulse with an interval of 10 s for total 5 min using an ultrasonicator probe (Vibra cell 75043). The suspension was then incubated for 4 h at room temperature. About 5 μl of this suspension was dropped on each sensor covering an area of 3 mm^2 that was previously activated with cysteamine SAM. The sensors were then incubated in an airtight humid chamber for 10 h for covalent attachment of carboxy-CNTs and rinsed with sterile distilled water. The free carboxyl groups on sensors were blocked by adding 5 μl of 50 mM ethanolamine and finally washed with 50% DMSO in water followed by acetone to remove traces of unbound CNTs and dried over N_2 gas. A sensor array without CNT immobilization was used as a control for comparison.

A modified 44-mer RNA aptamer that specifically bind CRP (Bini et al., 2008) was custom synthesized after modifying with alkane thiol-linker at the 5′ end. The ability of modified aptamer to bind CRP has been recently reported (Qureshi et al., 2010). The resulting modified RNA aptamer had the following sequence; 5′-HS-(CH2)6-GCCUGUAAGGUGGUCGGUGUGGCGAGUGUGUUAGGAGAGAUUGC-3′ and its complementary RNA strand (cRNA) used had the following sequence; 5′-GCAAUCUCUCCUAACACACUCGCCACA-CCGACCACCUUACAGGC-3′.

In order to determine the influence of the coverage on the overall response of the aptamers on the sensor surface, we initially conducted a preliminary test experiment with thiol-modified RNA aptamers directly immobilized on GID region of the sensor arrays by self-assembled monolayer (SAM) formation (Qureshi et al., 2010). For this, different concentrations of thiol-modified RNA aptamers (2 μl of 4, 6, and 10 μM) were incubating in phosphate buffered saline (PBS), pH 7.2 for 2 h at 25 °C, under sterile conditions. The immobilized RNA aptamer concentration (10 μM) that gave a significant change in dielectric responses (impedance/capacitance) was subsequently used to immobilize on all CNT activated sensor arrays in this study. The CNT activated GID regions of sensor arrays were immobilized with 10 μM modified RNA aptamer by physical adsorption in PBS for 2 h at 25 °C under sterile conditions (see SI section). After the adsorption of RNA aptamers, the sensors were thoroughly washed thrice with sterile distilled water and dried using N_2 gas and stored at 4 °C until use.

2.4. Surface characterization

The surface characterization was performed using Atomic Force Microscopy (AFM, Nanoscope) with the tapping mode. The surface topology of sensor surface was carried out with bare GID

surface, after activation with CNTs and after the physisorption of RNA aptamers. Average height and surface root mean square (RMS) roughness was calculated from the AFM images using WSxM 5.0 Develop 4.0 image browser.

2.5. Dielectric measurements (impedance/capacitance)

The dielectric properties in between the interdigitated electrodes were measured by non-Faradaic electrochemical impedance spectroscopy (nFEIS) in the frequency range 50 Hz–1 GHz using a Network Analyzer (Karl-Suss PM-5 RF Probe Station). The Network Analyzer was calibrated using SOLT (short-open-load-through) method. The impedance values were exported to MATLAB® program for the analysis. The capacitance values were extracted at an effective frequency (f) (200 MHz) and normalized with respect to blank and negative controls. The relative capacitance variations were calculated from the data obtained at 200 MHz frequency under standard assay conditions using Eq. (1) as described previously (de Vasconcelos et al., 2009).

$$\frac{C - C_0}{C_0} \times 100 \quad (1)$$

where C is the actual capacitance after the binding of the target CRP/cRNA with the RNA aptamer at a particular concentration and C_0 is the capacitance before binding. The average values of replicate experiments ($n = 3$) were plotted and the standard deviations are shown as error bars, and the relative standard deviation (RSD%) of 4–12%.

2.6. Binding specificity assay

A series of sensor arrays functionalized with the RNA aptamers were used for the binding specificity assays. First, pure forms and co-mixtures of CRP and cRNA in different ratios (1:0, 0:1, 1:1, 1:2 and 2:1) and at different concentrations (0–l2 μM equivalent to 0–7 μg/5 μl) were prepared in PBS. Non-specific molecules, such as bovine serum albumin (BSA) and a random ssDNA oligonucleotide (TCTAACGTCAATGATAGA-N40-TTAACTTATTCGACCAAA) were used as negative controls for CRP and cRNA, respectively. The sensor chips were incubated with the target and non-specific molecules (in 5 μl volume each) for 30 min at room temperature. The sensors were then washed twice with PBS and dried using N_2 gas and dielectric measurements were recorded.

2.7. Binding affinity assay

The sensors functionalized with aptamers were incubated with 0–12 μM pure and mixed forms of target CRP:cRNA targets in the ratio of 0:1 (pure cRNA), 1:0 (pure CRP), 1:1, 1:2, and 2:1 for 30 min. The unbound CRP/cRNA was removed by washing thrice with PBS and the sensors were dried. The capacitance values were measured under dry conditions and normalized. The binding data were fitted to determine the K_d values by non-linear regression analysis with the help of Eq. (2), using Sigmaplot 11.0 program (under ligand binding set to one site saturation mode).

$$y = \frac{B_{max}x}{K_d + x} \quad (2)$$

where y is degree of saturation, B_{max} is the number of maximum binding sites, x is the target concentration (cRNA/CRP), and K_d is the dissociation constant.

3. Results and discussion

3.1. Characterization of sensor surface

The carboxy-CNTs were immobilized covalently on cysteamine SAM layer of the sensor surface. RNA aptamers that specifically

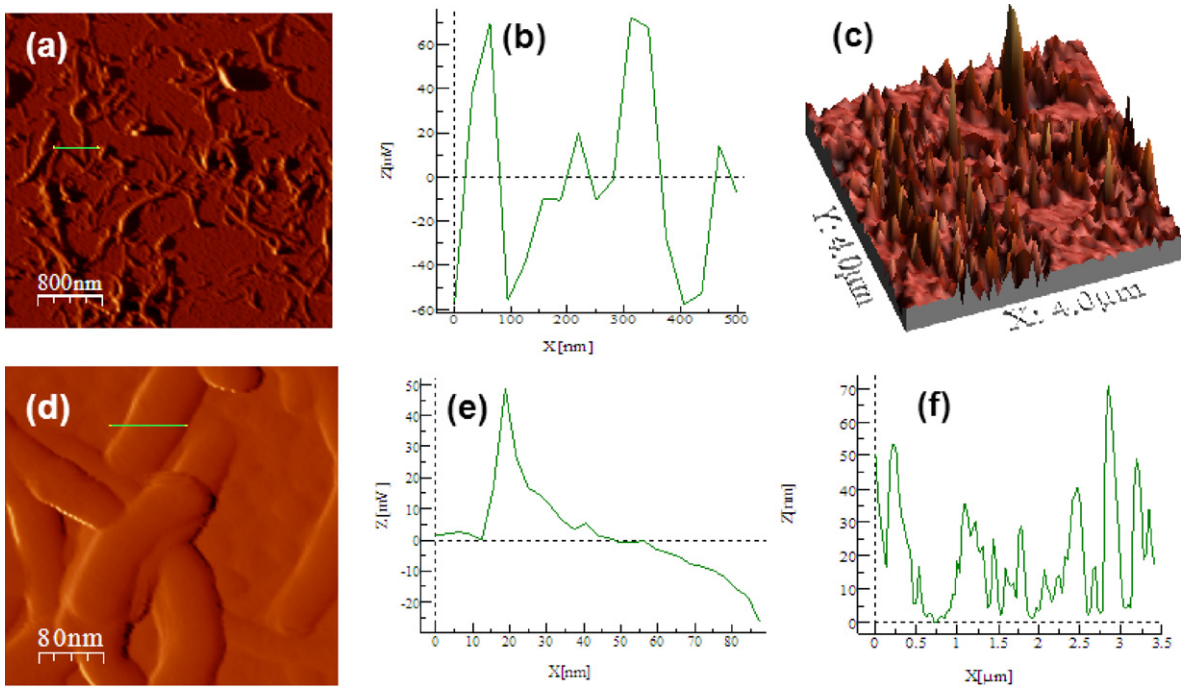

Fig. 1. Tapping-mode AFM images (within 4 μm × 4 μm scan area) of (a) GID surface activated with carboxy-CNTs, (b) line plot surface profile of the selected green line region (500 nm length) green highlighted in the AFM height image, (c) 3D AFM topographical map of carboxy-CNT activated surface, (d) a magnified AFM height image of GID surface activated with carboxy-CNTs within 400 μm × 400 μm scanned area of sensor surface activated with carboxy-CNTs, (e) Line plot surface profile of the selected line region (100 nm length) green highlighted in the AFM height image of GID electrode on sensor surface activated with carboxy-CNTs, and (f) surface topography and height analysis in 2D AFM image section (within 4 μm × 4 μm scan area) of GID surface activated with carboxy-CNTs. (For interpretation of the references to color in this figure legend, the reader is referred to the web version of the article.)

bind CRP were then allowed to physically adsorb onto the CNT activated sensor surface. The AFM images of sensor surface confirmed a random distribution of CNTs (Fig. 1a–f). A 3D height map displayed varying heights of CNTs within scanned 4 μm × 4 μm area of gold surface (Fig. 1c). The diameter of the immobilized bare CNTs was in 30–45 nm with an average surface RMS roughness of 48.55 nm (Fig. 1d–f). Activation of sensor surface with CNTs served primarily as the adsorption sites for RNA aptamers. In previous studies, CNTs have been used as an electrode material for supercapacitors because of their microscopic and macroscopic porous structures, electrochemical behavior, size and surface area, and provide large-charge storage capacity (An et al., 2001; Barisci et al., 2000; Tran et al., 2011; Yoon et al., 2004). Here, CNTs were utilized as binding surfaces for RNA aptamers as well as for space charge polarization at the electrode-nanotube interface under the applied AC-electrical frequency. Moreover, CNTs also possess superior power densities due to fast charging/discharging capabilities (An et al., 2001; Basu and Iannacchione, 2008). Adsorption of RNA aptamers on CNTs gave rise to an increase in diameter by 5–15 nm with an average surface RMS roughness changing from 48.55 nm to ~74 nm (Fig. S1a–f). Physical adsorption of RNA aptamers occurred by wrapping around the outer surfaces of CNTs by physical adsorption (Gowtham et al., 2008; Han et al., 2007; Yang et al., 2007). Thus, increase in the diameter of CNTs, and surface RMS roughness indicated the formation of RNA aptamer aggregates on the sensor surface (Fig. S1d), which is consistent to previously reported studies (Cabrera and Sanchez-Pomales, 2007; Yang et al., 2009). Further, it was found that the heights of RNA-aptamer bound CNTs were significantly enhanced with an average of 71 nm compared with only CNTs that had an average height of 45 nm on gold surface (Fig. 1d–f).

3.2. Aptamer–target binding and competition assay

A competition assay was designed for detection of target CRP based on bound/free separation of cRNAs by label-free capacitive method. RNA aptamers bind CRP by specific folding, which is induced by its target. These aptamers can also hybridize with complementary oligonucleotides (cRNA) to form duplex molecules. The competitive binding of RNA aptamers with either CRP or cRNA as targets in pure and co-mixed forms was analyzed by measuring the change in capacitance as shown in Scheme S2 of SI section.

Here, the RNA aptamers were physically adsorbed by wrapping on carboxy-CNT activated sensor surface (Scheme S1). The aptamer functionalized sensor surface was subjected to incubation with targets and probed the interaction of targets on the sensor surface. The target induced separation/dissociation of adsorbed aptamers is postulated to occur as a result of binding to target in free forms and thus enable determining the target concentration. To test this hypothesis, different concentrations (0–12 μM) and micromolar ratios of CRP:cRNA (0:1, 1:0 1:1, 1:2, and 2:1) were incubated on constant number of RNA-aptamers (10 μM) immobilized on sensor surface. The change in relative capacitance induced by the interaction of the aptamers with target molecules (CRP and/or cRNA) was measured by nFEIS, an advancement in label-free method for probing molecular interactions. The preferential binding ability of RNA aptamer with either of target molecules was determined, and the concentration dependent change in relative capacitance was measured as a function of applied AC frequency (at 200 MHz) (Fig. 3). The results showed that binding of RNA-aptamer to pure forms of CRP and cRNA molecules (1:0 and 1:0, respectively) exhibited distinct level of capacitance responses that was consistent to the distinct nature of target molecules that induced capacitance change. It was observed that higher charge distribution occurred as a result of interaction of pure cRNA as target molecules on sensor surface, yielding high capacitance change as compared with

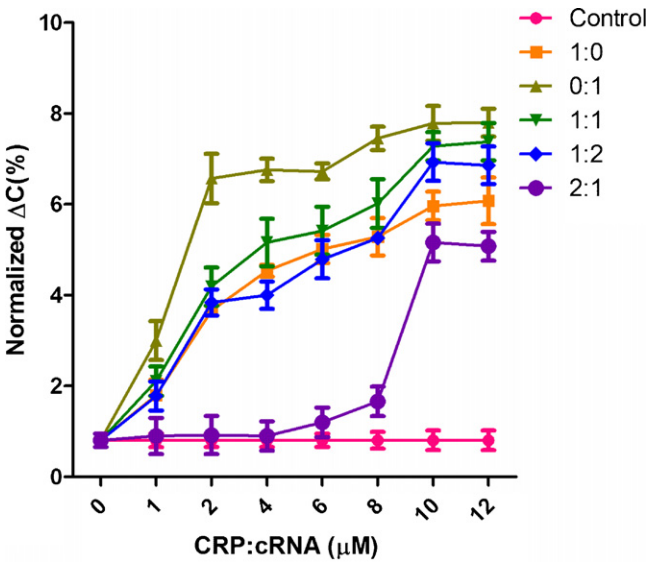

Fig. 2. Concentration dependent change in capacitive responses obtained with CNT activated sensor immobilized with RNA-aptamers that bind to CRP or cRNA target molecules. The target molecules were incubated on sensor surface in pure forms and in co-mixtures in different concentrations and ratios indicated in the figure legends.

binding of pure CRP (Fig. 2). This large capacitance change with cRNAs could be attributed to its relatively small size (~14 kDa) compared to CRP (~115.13 kDa) combined with charge distribution derived from the negative charges of the duplex cRNA-aptamer backbone. On the other hand, the interaction of the immobilized RNA aptamers with CRP yielded half the response seen with cRNA (Fig. 3).

The reduced response level with CRP target can be attributed to the following plausible reasons; (a) separation or dissociation of the adsorbed aptamers occurred probably by CRP induced secondary folding of aptamer, an essential feature of aptamers for binding to their target proteins, and (b) partial or complete dissociation of aptamers driven by excess free CRP target. The

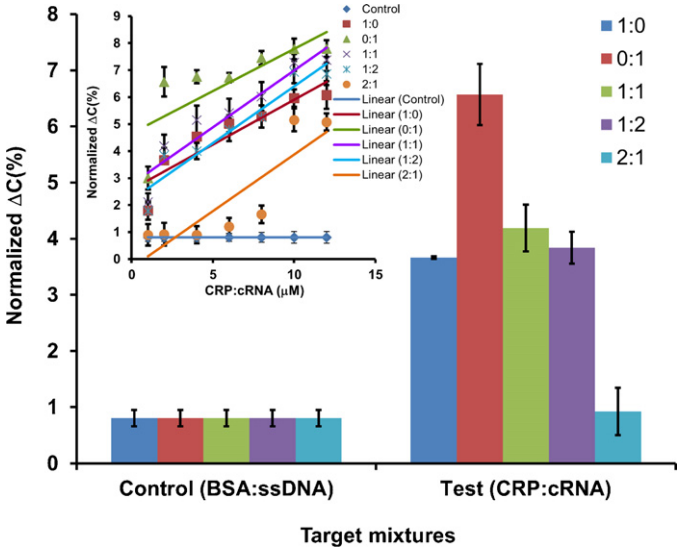

Fig. 3. Response of sensor at a constant concentration (2 μM) of targets against different CRP:cRNA ratios that are indicated in the legend. The inset figure shows linear regression lines plotted with concentration dependent responses with different ratios of CRP/cRNA in pure and co-mixtures.

above assumption was further evidenced by the response obtained with target mixtures of CRP:cRNA in the ratio of 2:1 to which the sensor response dramatically declined or showed negligible response (Fig. 3). Here, the immobilized aptamers interacted with either of the targets (CRP or cRNA) giving rise to the formation of an aptamer–target complex. As a result of probe–target interactions, changes occurred in the aptamers' conformation that induced separation/dissociation from the sensor surface and thus collective charge distribution on the chip surface was dramatically dropped. This enabled determining the target CRP/cRNA concentrations based on bound/free target separation. It was found that the detection limit for CRP was 1–8 μM (0.58–4.6 μg/5 μl volume sample on each capacitor) (Fig. 3 inset) and this level for CRP falls well within the normal clinical levels (1–3 mg/ml) (Pearson et al., 2003). In a previous report, the aptamers were immobilized chemically as opposed to physical adsorption on sensor surface, and thus, the bound complex remained on sensor surface, which gives rise to sensitive change in the signal (Qureshi et al., 2010). For a negative control, a non-specific BSA protein and random ssDNA oligonucleotides were tested in place of targets CRP and cRNA, respectively that showed no change in responses, suggesting that the sensor was specific to its target molecules (Fig. 3).

The capacitive responses obtained as a result of interaction of aptamer–target molecules with different target ratios were plotted. It was found that at 2 μM initial concentration of targets tested showed maximum capacitive responses compared with that of higher concentrations (4–12 μM) (Figs. 2 and 3) probably because lower target concentration causes less charge distribution when compared to higher concentrations. The greater the concentration of target molecules the lower the capacitance change occurred. The capacitive response for the pure cRNA (CRP:cRNA = 0:1) was greater than that found with the pure CRP (CRP:cRNA = 1:0). This implies that RNA aptamers may prefer binding to its complementary RNA strand (cRNA) over binding to CRP. While in case of co-incubation of different CRP:cRNA ratios, the capacitance change remained nearly same as that of pure CRP. The capacitance change for equimolar CRP:cRNA (1:1) being similar to pure CRP (1:0) suggests that the binding of CRP prevailed over the binding of cRNA. Further, there was no significant increase in capacitance when the concentration of cRNA was greater than that of CRP (0:1 and 1:2, CRP:cRNA) probably because of tight competition between the two targets for binding to RNA aptamer. These results imply that hybridization of RNA aptamer with cRNA at higher CRP concentrations did not yield significant responses.

It was observed that the variation in the relative capacitance responses at applied frequency (200 MHz) was dependent on the concentration of target ratios (Figs. 2 and 3 inset). The differences and the sensitivity in response to different target ratios under the applied frequency could be strongly dependent on the dominant nature of one type of target, either CRP or cRNA depending upon their competition to bind the probe molecules as well as the specific geometry of gold electrodes (Dobrikova et al., 2007; Song, 2002).

Binding kinetics as determined by incubating different target concentrations against constant number of aptamers immobilized on sensor surface showed the K_d values of 1.98 and 2.4 μM for cRNA and CRP, respectively. The K_d values indicated that the binding affinity with pure cRNA was stronger than the pure CRP molecules. Further, it is noted that binding affinity reduced with CRP:cRNA co-mixtures of 1:1 (K_d = 2.86 μM), 1:2 (K_d = 3.8 μM) and 2:1 (K_d = 8.58 μM) probably because of the strict competition to bind between the target molecules. The high K_d for 2:1 ratio is consistent with drop in sensor signal as it implies dissociation of the immobilized aptamers from the sensor surface influenced by excess CRP (Fig. 3).

4. Conclusions

This paper reports on a new approach to study molecular interactions in native forms of biomolecules without the use of any interfering agents. To our knowledge, this is a first report on competitive assay based on capacitance change that has a great potential to study the molecular interactions of various other probe and target molecules. Here, RNA aptamers served as probe elements to which target CRP and/or cRNA competitively interacted when incubated in pure forms and in co-mixtures in different ratios. The CNTs on sensor surface played a dual role of enhancing the capacitive signal, and serve as active binding surfaces for physical adsorption of aptamers. Binding kinetic results showed that the immobilized aptamers had strong affinity to bind pure cRNA/CRP. The aptamers tend to dissociate from the sensor in presence of excess CRP in a complex CRP:cRNA mixture. Based on this separation/dissociation, free CRP concentration was determined and the detection limit was 1–8 μM (0.115–1.15 mg/l), which is well within the normal clinical levels (1–3 mg/l). The presented aptamer-based, label-free capacitive method has a great potential that offers advantages of speed, simplicity and sensitivity for detection of biomolecules. However, there are a few challenges, such as (a) improving the sensitivity through better design and geometry of electrodes in nano-sizes, (b) integrating microfluidics for small volume sample handling and (c) portability are the current challenges that are aiming to accomplish in this laboratory.

Acknowledgments

This work was supported by the Scientific and Technological Research Council of Turkey (TUBITAK) 1001 grant no. 110E287. We thank Saravan Kallempudi, Samet Zaheer, Bulent Koroglu, Ali Kasal and Mehmet Dogan for helping with chip fabrication/processing and measurements. We also thank the Materials Science and Engineering program of the Faculty of Engineering and Natural Sciences, Sabanci University for the Atomic Force Microscopy.

Appendix A. Supplementary data

Supplementary data associated with this article can be found, in the online version, at doi:10.1016/j.bios.2012.01.038.

References

An, K.H., Kim, W.S., Park, Y.S., Choi, Y.C., Lee, S.M., Chung, D.C., Bae, D.J., Lim, S.C., Lee, Y.H., 2001. Adv. Mater. 13, 497–500.
Bagalkot, V., Farokhzad, O.C., Langer, R., Jon, S., 2006. Angew. Chem. Int. Ed. Engl. 45, 8149–8152.
Barisci, J.N., Wallace, G.G., Baughman, R.H., 2000. J. Electrochem. Soc. 147, 4580–4583.
Basu, R., Iannacchione, G.S., 2008. J. Appl. Phys. 104, 114107.
Berezovski, M., Sergey, N., 2003. J. Am. Chem. Soc. 125, 13451.
Bini, A., Centi, S., Tombelli, S., Minunni, M., Mascini, M., 2008. Anal. Bioanal. Chem. 390, 1077–1086.
Cabrera, C.R., Sanchez-Pomales, G., 2007. J. Electroanal. Chem. 606, 47–54.
Casas, J., Shah, T., Hingorani, A., Danesh, J., Pepys, M., 2008. J. Int. Med. 264, 295.
Chiu, T.C., Huang, C.C., 2009. Sensors 9, 10356.
de Vasconcelos, E.A., Peres, N.G., Pereira, C.O., da Silva, V.L., da Silva Jr., E.F., Dutra, R.F., 2009. Biosens. Bioelectron. 25, 870–876.
Dobrikova, A.G., Dimitrov, M.I., Taneva, S.G., Petkanchin, I.B., 2007. Colloids Surf. B Biointerfaces 56, 114–120.
Foulds, G.J., Etzkorn, F.A., 1998. Nucleic Acids Res. 26, 4304–4305.
Gautier, C., Esnault, C., Cougnon, C., Pilard, J.F., Casse, N., Chenais, B., 2007. J. Electroanal. Chem. 610, 227–233.
Gowtham, S., Scheicher, R.H., Pandey, R., Karna, S.P., Ahuja, R., 2008. Nanotechnology 19, 125071.
Han, X.G., Li, Y.L., Deng, Z.X., 2007. Adv. Mater. 19, 1518–1522.
Hansen, J.A., Wang, J., Kawde, A.N., Xiang, Y., Gothelf, K.V., Collins, G., 2006. J. Am. Chem. Soc. 128, 2228–2229.
Karlsson, R., 2004. J. Mol. Recognit. 17, 151–161.
Laczka, O., Baldrich, E., Mun oz, F., del Campo, F., 2008. Anal. Chem. 80, 7239–7247.

Lei, L.H., Fu, Y.C., Xu, X.H., Xie, Q.J., Yao, S.Z., 2009. Prog. Chem. 21, 724–731.
Mukhopadhyay, R., 2005. Anal. Chem. 77, 114–118.
Pagano, J.M., Clingman, C.C., Ryder, S.P., 2011. RNA 17, 14–20.
Pearson, T.A., Mensah, G.A., Alexander, R.W., Anderson, J.L., Cannon 3rd, R.O., Criqui, M., Fadl, Y.Y., Fortmann, S.P., Hong, Y., Myers, G.L., Rifai, N., Smith Jr., S.C., Taubert, K., Tracy, R.P., Vinicor, F., 2003. Circulation 107, 499–511.
Quershi, A., Gurbuz, Y., Kang, W.P., Davidson, J.L., 2009. Biosens. Bioelectron. 25, 877–882.
Qureshi, A., Gurbuz, Y., Kallempudi, S., Niazi, J.H., 2010. Phys. Chem. Chem. Phys. 12, 9176–9182.
Royer, C.A., Scarlata, S.F., 2008. Methods Enzymol. 450, 79–106.
Ryder, S.P., Recht, M.I., Williamson, J.R., 2008. Methods Mol. Biol. 488, 99–115.
Sassolas, A., Blum, L.J., Leca-Bouvier, B.D., 2009. Electroanalysis 21, 1237–1250.
Singhal, R.P., Otim, O., 2000. Biochem. Biophys. Res. Commun. 272, 251–258.
Song, X.Y., 2002. J. Chem. Phys. 116, 9359–9363.
Strehlitz, B., Nikolaus, N., Stoltenburg, R., 2008. Sensors 8, 4296–4307.
Tlili, C., Korri-Youssoufi, H., Ponsonnet, L., Martelet, C., Jaffrezic-Renault, N.J., 2005. Talanta 68, 131–137.
Tran, L.D., Nguyen, D.T., Nguyen, B.H., Do, Q.P., Nguyen, H.L., 2011. Talanta 85, 1560–1565.
Varshney, M., Li, Y., Srinivasan, B., Tung, S., 2007. Sens. Actuat. B Chem. 128, 99–107.
Velasco-Garcia, M.N., Missailidis, S., 2009. Gene Ther. Mol. Biol. 13, 1–9.
Wan, Q.H., Le, X.C., 2000. Anal. Chem. 72, 5583–5589.
Wang, W.J., Chen, C.L., Qian, M.X., Zhao, X.S., 2008. Anal. Biochem. 373, 213–219.
Wong, I., Lohman, T.M., 1993. Proc. Natl. Acad. Sci. U.S.A. 90, 5428–5432.
Xu, Y., Cheng, G.F., He, P.G., Fang, Y.Z., 2009. Electroanalysis 21, 1251–1259.
Yang, Q.H., Gale, N., Oton, C.J., Li, F., Vaughan, A., Saito, R., Nandhakumar, I.S., Tang, Z.Y., Cheng, H.M., Brown, T., Loh, W.H., 2007. Nanotechnology 18, 405706.
Yang, Q.H., Wang, Q., Gale, N., Oton, C.J., Cui, L., Nandhakumar, I.S., Zhu, Z.P., Tang, Z.Y., Brown, T., Loh, W.H., 2009. Nanotechnology 20, 195603.
Yoon, B.J., Jeong, S.H., Lee, K.H., Kim, H.S., Park, C.G., Han, J.H., 2004. Chem. Phys. Lett. 388, 170–174.